Exciton dipole-dipole interaction in a single coupled-quantum-dot structure via polarised excitation

Heedae Kim,[†,‡] Inhong Kim,[†] Kwangseuk Kyhm,[*,†] Robert A. Taylor,[*,‡] Jong Su Kim,[¶] Jin Dong Song,[§] Koo Chul Je,[‖] and Le Si Dang[⊥]

[†]*Department of Opto-mechatronics and Cogno-mechatronics, RCDAMP, Pusan Nat'l University, Busan 609-735, Republic of Korea*

[‡]*Clarendon Laboratory, Department of Physics, University of Oxford, Oxford, OX1 3PU, U.K*

[¶]*Department of Physics, Yeungnam University, Gyeongsan, 712-749, Republic of Korea*

[§]*Nano-Photonics Research Center, KIST, Seoul, 136-791, Republic of Korea*

[‖]*College of Liberal Arts and Sciences, Anyang University, Gyeonggi-do 430-714, South Korea*

[⊥]*Department of NANOscience, Institut Néel, CNRS, rue des Martyrs 38054, Grenoble, France*

E-mail: kskyhm@pusan.ac.kr; robert.taylor@physics.ox.ac.uk

Abstract

We find that the exciton dipole-dipole interaction in a single laterally-coupled GaAs/AlGaAs quantum dot structure can be controlled by the linear polarisation of a non-resonant optical excitation. When the excitation intensity is increased with the linearly polarised light parallel to the lateral coupling direction [$1\bar{1}0$], excitons (X_1 and X_2) and local

biexcitons (X_1X_1 and X_2X_2) of the two separate quantum dots (QD_1 and QD_2) show a redshift along with coupled biexcitons (X_1X_2), whilst neither coupled biexcitons nor a redshift are observed when the polarisation of the exciting beam is perpendicular to the coupling direction. The polarisation dependence and the redshift are attributed to an optical nonlinearity in the exciton Förster resonant energy transfer interaction, whereby exciton population transfer between the two quantum dots also becomes significant with increasing excitation intensity. We have further distinguished coupled biexcitons from local biexcitons by their large diamagnetic coefficient.

keywords: Laterally-coupled quantum dot structures, dipole-dipole interaction, FRET, coupled biexcitons.

Introduction

As building-blocks of quantum bits, various coupled quantum dot (CQD) structures have been studied in terms of coupling and entangling of quantum states.[1–9] When the inter-dot distance of a CQD is short enough ($d < 10\,\mathrm{nm}$) to result in a wavefunction overlap between the two quantum dots (QDs) via the tunnelling effect, the optimal coupling is controlled by the inter-dot distance and any external DC electric field along the coupling direction.[10–19] When the eigenstates of CQDs are measured by the photoluminescence of an electron-hole pair in the presence of an external electric field, indirect electron-hole pairs can also be involved, where the electrons and the holes belong to different QDs. As a result, the indirect and direct electron-hole pairs of a CQD structure give rise to both symmetric and anti-symmetric eigenstates.[18,19] This scheme was mainly applied to vertically stacked QDs, where the electric field is applied vertically. Although charge injection was induced in a laterally CQD[11,12] by applying an external DC-electric field, wavefunction overlap was not achieved. Furthermore, this electrically-induced coupling technique requires extra fabrication processes and the preparation of electrodes. If optically-induced coupling between QDs

is possible, the system can be simplified.

When the separation of two QDs is not small enough to give rise to a sufficient wavefunction overlap for tunneling to occur, the exciton dipole-dipole interaction can be used as an alternative method of coupling two separate QDs.[20] Recently, exciton dipole-dipole interactions in colloidal quantum dots were used for bio-sensing and solar cell applications, where the optimum inter-dot distance is important for efficient population transfer and exciton transport.[15] However, the exciton dipole-dipole interaction also depends on other parameters such as the relative dipole orientation, permanent dipole strength, and donor-acceptor energy difference, and these parameters need to be studied rigorously in a well-defined single nanostructure. Excitonic dipole-dipole interaction in CQD structures has been studied in interface QDs formed in a thickness fluctuating quantum well, where a transient exciton-exciton interaction was observed on a picosecond timescale.

Although resonant excitation can be used to set the orientation of an exciton dipole, the ground exciton state is limited by a small absorption cross section. However, as long as the excited state spin is maintained during intra-relaxation toward the ground state, optical non-resonant spin injection can be used in a manner similar to electrical spin injection. In this work, we have found that the exciton dipole-dipole interaction in a single lateral coupled-quantum-dot depends strongly on the orientation of the linear polarisation of non-resonant laser excitation. When this non-resonant excitation is polarised along the coupling direction of a CQD, a coupled biexciton (X_1X_2) consisting of different excitons from two separate QDs (QD_1 and QD_2) can be generated selectively, and exciton population transfer occurs from the smaller QD (QD_1) to the larger QD (QD_2).

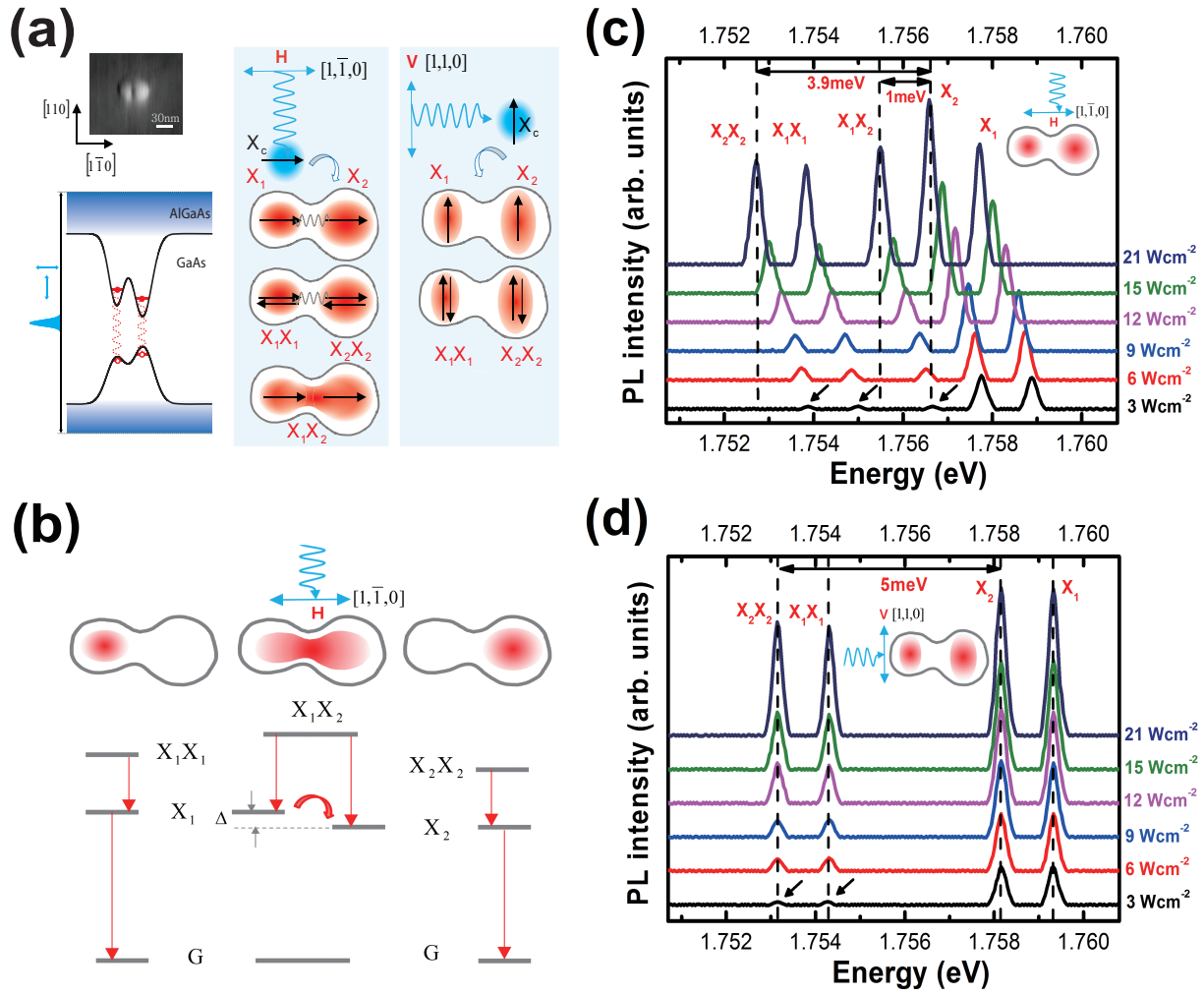

Figure 1: **(a)** AFM image and schematic confinement potential energy of a single lateral coupled-quantum-dot. Excitons (X_1 and X_2) and local biexcitons (X_1X_1 and X_2X_2) can be generated separately in the two different GaAs QDs (QD_1 and QD_2) through the continuum exciton (X_c) states in the AlGaAs barrier or the intra-relaxation of individual free electrons and holes. When the non-resonant excitation intensity is polarised along [1$\bar{1}$0] (denoted by H) increases, a coupled biexciton (X_1X_2) also appears. **(b)** Due to an energy difference ($\Delta_{12} \simeq 1\,\text{meV}$) between X_1 and X_2, X_1X_2 can show a doublet spectrum with the same separation ($\simeq 1\,\text{meV}$) as a consequence of the two transitions, $X_1X_2 - X_1$ and $X_1X_2 - X_2$. **(c)** While the transition of $X_1X_2 - X_1$ is observed, the $X_1X_2 - X_2$ transition happens to be overlap spectrally with the X_2 PL emission. A redshift is also observed for all of the coupled biexcitons, local biexcitons, and excitons. **(d)** Increasing the non-resonant excitation intensity for light polarised perpendicular to the coupling direction [110] (denoted by V), produces no visible coupled biexcitons nor are any redshifts observed.

Results and discussion

Fig.1(a) shows an AFM image of an uncapped GaAs CQD, where the dimensions along $[1\bar{1}0]$ and [110] are $\sim 60\,\mathrm{nm}$ and $\sim 44\,\mathrm{nm}$ respectively, and the two different QDs are coupled along the $[1\bar{1}0]$ direction. The height of QD_1 ($\sim 4.5\,\mathrm{nm}$) is also slightly lower than that of QD_2 ($\sim 5.2\,\mathrm{nm}$), and the top-top distance is $\sim 26\,\mathrm{nm}$. Because of the morphology, the confinement potential of a GaAs/AlGaAs CQD can be illustrated by the schematics in Fig.1(a), where QD_1 has a large energy difference between the minimum confinement potential energy of the conduction and valence bands, and its potential parabola is also stiff compared to QD_2. Therefore the different energy levels of separate excitons (X_1 and X_2) in the two different quantum dots can be resolved spectrally (Supporting Information).

Because of the lateral shape asymmetry of a CQD, the exciton eigenstates can be accessed by using linearly polarised light, aligned parallel or perpendicular to the lateral coupling direction $[1\bar{1}0]$. As a charge displacement between the electron and hole is induced along the linear polarisation, an associated dipole-dipole interaction should be produced, which depends on the relative orientation between the exciton dipoles on separate QDs. As the attractive interaction is maximized when the two exciton dipoles are aligned along the $[1\bar{1}0]$ direction, a coupled biexciton (X_1X_2) consisting of the different excitons (X_1 and X_2) can be generated with polarised light excitation parallel to the $[1\bar{1}0]$ direction. On the other hand, the exciton dipole-dipole interaction would be weaker when the dipoles are aligned along [110].

An exciton dipole oriented along the preferential direction $[1\bar{1}0]$ can be induced directly by using linearly polarised resonant light. However, linearly polarised non-resonant light can also be used provided that the spin coherence of an electron and a hole is maintained during the intra-relaxation, where the linear polarisation gives rise to a superposition of exciton spin-up ($+\hbar$) and -down states ($-\hbar$). A whole exciton can relax from the barrier to the ground state of a QD, but individual relaxation of hot electrons and holes is also possible. When the electron-hole exchange interaction becomes involved in the former process, the

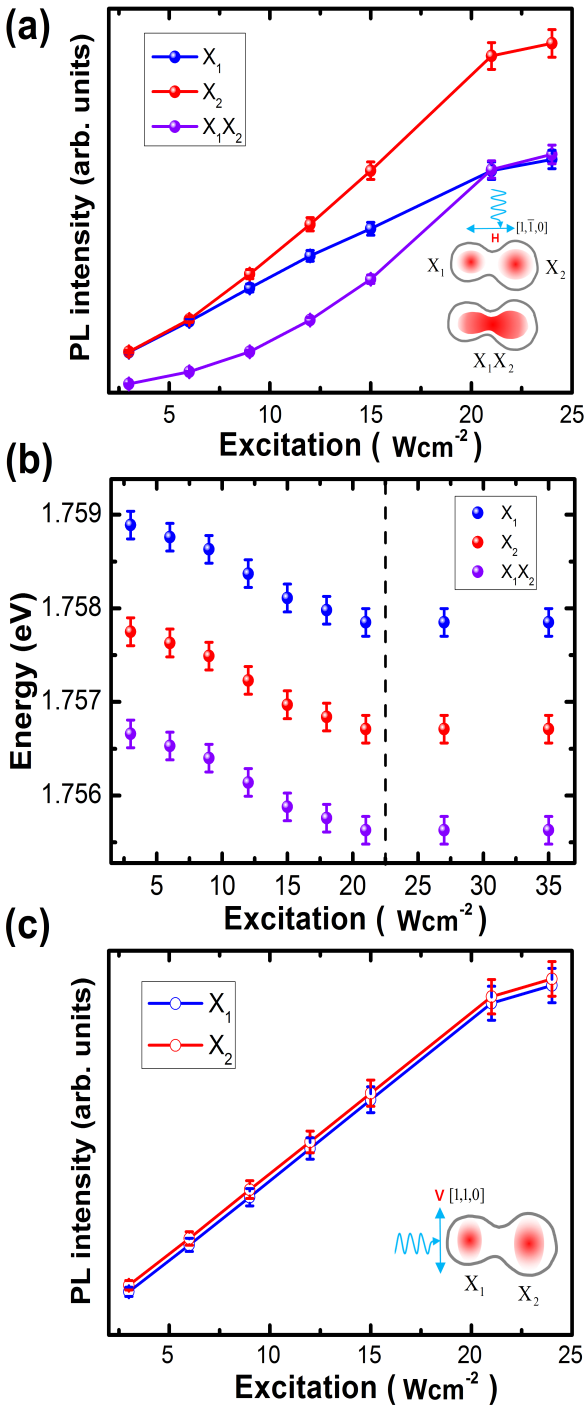

Figure 2: When the polarised excitation intensity parallel to $[1\bar{1}0]$ (denoted by H) increases, the integrated-PL intensity of X_2 becomes enhanced gradually compared to that of X_1. Meanwhile the coupled biexciton (X_1X_2) also becomes significant **(a)**, and X_1, X_2, and X_1X_2 all show a redshift up to the saturation excitation intensity ($\sim 22\,\mathrm{Wcm}^{-2}$) **(b)**. On the other hand, with increasing polarised excitation intensity parallel to [110] (denoted by V), the integrated-PL intensities of X_1 and X_2 are balanced and increase linearly without any spectral shift **(c)**.

spin coherence is merely transferred to the ground state of the QD. On the other hand, the spin relaxation is relatively inefficient in the latter case.[21,22] The discrete energy levels of QDs are also beneficial for spin coherence as the spin-orbit interaction is inhibited. As shown in Fig.1(c,d), a significant difference is apparent between the PL spectra for polarised non-resonant excitation parallel to $[1\bar{1}0]$ (denoted by H) and that parallel to [110] (denoted by V). As the intensity of the V excitation is increased, local biexcitons (X_1X_1 and X_2X_2) and the corresponding excitons (X_1 and X_2) are observed, but no spectral shift is seen. On the other hand, as the intensity of the H excitation is increased, an additional PL peak appears between X_1X_1 and X_2, which is associated with X_1X_2. As the different excitons (X_1 and X_2) are bound across separate QDs, the binding energy of X_1X_2 is small compared to that of the local biexcitons ($\sim 3.9\,\mathrm{meV}$), where the both X_1X_1 and X_2X_2 have a similar binding energy. We also note that the binding energy of the local biexcitons generated by V-polarisation is relatively large ($\sim 5\,\mathrm{meV}$)[23] possibly due to the relatively small confinement size along [110] (Fig.1(d)). The energy difference ($\Delta_{12} \simeq 1\,\mathrm{meV}$) between X_1 and X_2, X_1X_2 should show a doublet PL spectrum with the same separation ($\simeq 1\,\mathrm{meV}$) as a consequence of the two transitions, $X_1X_2 - X_1$ and $X_1X_2 - X_2$ as shown in Fig.1(b). Therefore, the additional PL peak between X_1X_1 and X_2 (Fig.1(c)) can be attributed to the $X_1X_2 - X_1$ transition, but the other transition $X_1X_2 - X_2$ overlaps with the X_2 PL spectrum. The biexcitonic nature of the peak has been confirmed further in terms of a super-linear PL intensity growth with excitation intensity (I_{ex}) at X_1X_2 ($\sim I_{\mathrm{ex}}^{2.1}$), X_1X_1 ($\sim I_{\mathrm{ex}}^{2.0}$), and X_2X_2 ($\sim I_{\mathrm{ex}}^{2.1}$) (Fig.2(a) and Supporting Information).

Interestingly, with increasing H-polarised excitation power, a super-linear growth of the PL intensity is observed at X_2 ($\sim I_{\mathrm{ex}}^{1.4}$). The excitation dependence of the X_1 PL intensity also deviates from a linear dependence ($\sim I_{\mathrm{ex}}^{0.9}$). Additionally, a redshift is significant in all the PL spectra of coupled biexcitons, local biexcitons, and excitons (Fig.2(b)) up to the saturation excitation intensity ($\sim 22\,\mathrm{Wcm}^{-2}$). In contrast, increasing the V-polarised non-resonant excitation intensity, produces balanced PL intensities for both X_1 and X_2, which

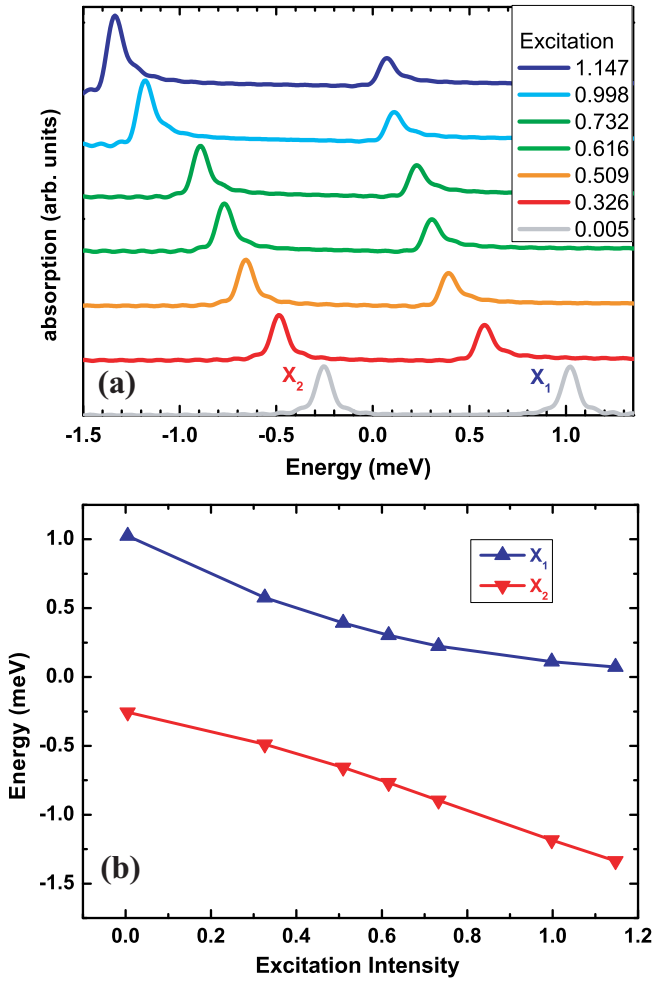

Figure 3: Theoretical exciton absorption spectrum (X_1 and X_2) **(a)** and energy shift **(b)** of QD_1 and QD_2 with increasing normalised H-polarised excitation power.

increase linearly ($\sim I_{ex}^{1.0}$) (Fig.2(c)), and no spectral shift is observed in the PL emission energy of local biexcitons and excitons (Fig.1(d)). Therefore, the emergence of a redshift and coupled biexcitons is most probably associated with an attractive dipole-dipole interaction between the two exciton dipoles aligned along the coupling direction $[1\bar{1}0]$ via H-polarised non-resonant excitation. Since the X_2 emission is spectrally overlapped with that of the $X_1X_2 - X_2$, the coupled biexciton may contribute to the super-linear PL intensity dependence of X_2 ($\sim I_{ex}^{1.4}$). Alternatively, an exciton population transfer[24,25] from X_1 to X_2 can also be a possible cause.

In order to explain the redshift with increasing H-polarised excitation intensity (Fig.1(c)),

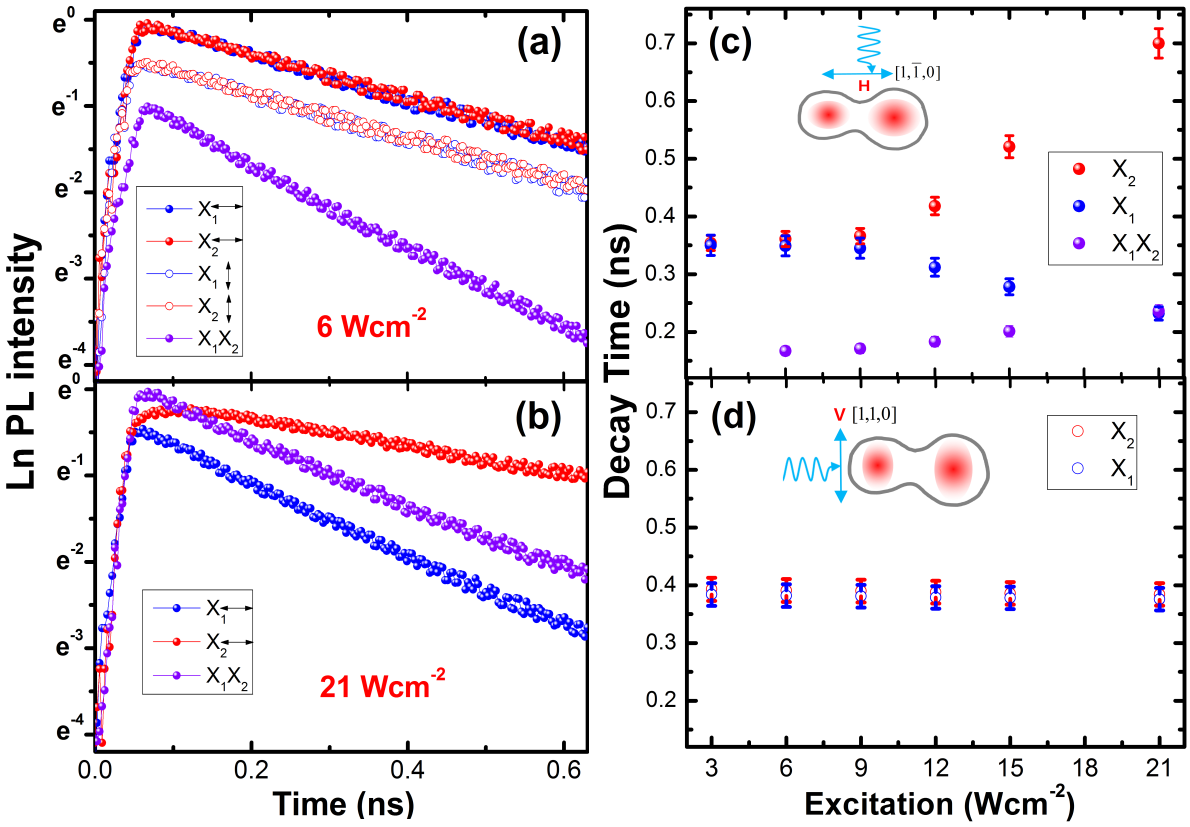

Figure 4: Time-resolved PL intensity measured with weak ($6\,\mathrm{Wcm^{-2}}$) **(a)** and strong ($21\,\mathrm{Wcm^{-2}}$) excitation intensity **(b)**, where the filled and open circles are of H- ($\leftrightarrow$) and V-polarised ($\updownarrow$) excitation respectively. **(c,d)** Excitation power dependence of PL decay time are plotted for H- and V-polarised excitation, which are parallel to $[1\bar{1}0]$ and $[110]$ respectively.

we have considered the optical nonlinearity theoretically in terms of the excitation dependent absorption spectrum of a CQD when the parallel exciton dipoles of QD_1 and QD_2 are aligned to the H-direction under excitation of a Gaussian laser pulse with $\sim 2.2\,\mathrm{meV}$ spectral width (Supporting Information). As shown in Fig.3 (a), significant redshift appears with increasing H-polarised excitation, but we found no spectral shift for increasing V-polarised excitation. In the case of H-polarised excitation, the coupling strength of the FRET interaction $V_{\mathrm{F}}^{\mathrm{H}} = -1.24\,\mathrm{meV}$ is found to be large compared to that of the direct Coulomb dipole interaction $V_{\mathrm{D}}^{\mathrm{H}} = +0.81\,\mathrm{meV}$, whilst the both are comparable for V-polarisation, i.e., $V_{\mathrm{F}}^{\mathrm{V}} = -0.35\,\mathrm{meV} \sim V_{\mathrm{D}}^{\mathrm{V}} = +0.40\,\mathrm{meV}$. Therefore, the redshift with increasing H-polarised excitation can be dominated by FRET. On the other hand, in the case of V-polarisation, the redshift due to the FRET interaction is compensated by the blueshift due to the direct Coulomb dipole interaction. Our theoretical energy shift up to the saturation excitation in Fig.3(b) is also comparable to the experimental redshift ($\sim 1\,\mathrm{meV}$). In the case of interface QDs localised in a quantum well, it was reported that the FRET interaction becomes suppressed due to a level repulsion effect in a disordered system, and the dominant direct Coulomb dipole interaction results in a transient blueshift. However, in our lateral coupled-quantum-dot system this is not the case, where FRET plays a dominant role in the dipole-dipole interaction along the preferential orientation.

As shown in Fig. 4(a), with low excitation ($\sim 6\,\mathrm{Wcm^{-2}}$), the exciton PL decay time with H-polarised excitation is slightly shorter ($\sim 350\,\mathrm{ps}$) than that with V-polarised excitation ($\sim 390\,\mathrm{ps}$). Given that the exciton PL energy for H-polarised excitation is lower than that for V-polarised excitation (Fig.1 (c,d)), the oscillator strength for a H-polarised exciton is probably larger than that for a V-polarised exciton due to the difference in the confinement size. The fast PL decay times of X_1X_1, X_2X_2, and X_1X_2 also confirm their biexciton nature, particularly given the super-linear dependence of the PL intensity with excitation power (Fig.2(a) and Supporting Information).[26] However, with increasing H-polarised excitation power (Fig. 4(b,c)) the PL decay times of X_1 and X_2 were observed to decrease and increase

respectively, whilst the PL decay time difference for X_1 and X_2 is small at low excitation power ($\sim 6\,\mathrm{Wcm}^{-2}$). In contrast, the PL decay times of X_1 and X_2 remain constant with increasing V-polarised excitation (Fig. 4(d)), which is consistent with the balanced PL emission intensity of X_1 and X_2 as the excitation power is increased (Fig. 2(c)).

When considering the exciton population transfer from QD_1 to QD_2, the FRET rate ($k_F \sim \kappa^2$) also depends on the relative orientation of the two dipoles, which is described by a dipole orientation factor (κ).[27,28] For example, when two dipoles are perpendicular to each other, the FRET rate becomes zero ($\kappa = 0$). On the other hand, when the two exciton dipoles of QD_1 and QD_2 are aligned along $[1\bar{1}0]$, the FRET rate becomes maximized with $\kappa^2 = 4$, which is four times larger than the case of two dipoles both aligned along the [110] direction ($\kappa^2 = 1$). Therefore, the dynamic population imbalance (Fig. 4(b)) and the super-linear PL intensity of X_2 ($\sim I_{ex}^{1.4}$) with excitation power (Fig. 2(a)) result from an exciton population transfer from X_1 to X_2, and the excitation-dependent exciton PL decay time for H-polarised excitation (Fig.4(c)) can be attributed to the optical nonlinearities of the exciton FRET interaction, which become significant with the preferential alignment of two dipoles along $[1\bar{1}0]$.

Provided that one of the coupled biexciton transitions ($X_1X_2 - X_2$) overlaps spectrally with the X_2 PL emission, this can also be associated with the increase of the X_2 PL decay time with increasing H-polarised excitation power (Fig. 4(c)). In this case, the coupled biexciton ($X_1X_2 - X_1$) and local biexciton ($X_1X_1 - X_1$) transitions may compete to feed the X_1 population as shown schematically in Fig. 1(b). Interestingly, with increasing H-polarised excitation power, we found the decay time of the local biexciton PL ($X_1X_1 - X_1$ and $X_2X_2 - X_2$) decreases, but the decay time of $X_1X_2 - X_1$ transition increases. In contrast, the decay times of local biexcitons barely change with increasing V-polarised excitation power (Supporting Information). Consequently, as the H-polarised excitation power increases, the decay of local biexcitons ($X_1X_1 - X_1$ and $X_2X_2 - X_2$) becomes significantly rapid when compared to that of the coupled biexciton transitions ($X_1X_2 - X_1$ and $X_1X_2 - X_2$). Because the X_2 population

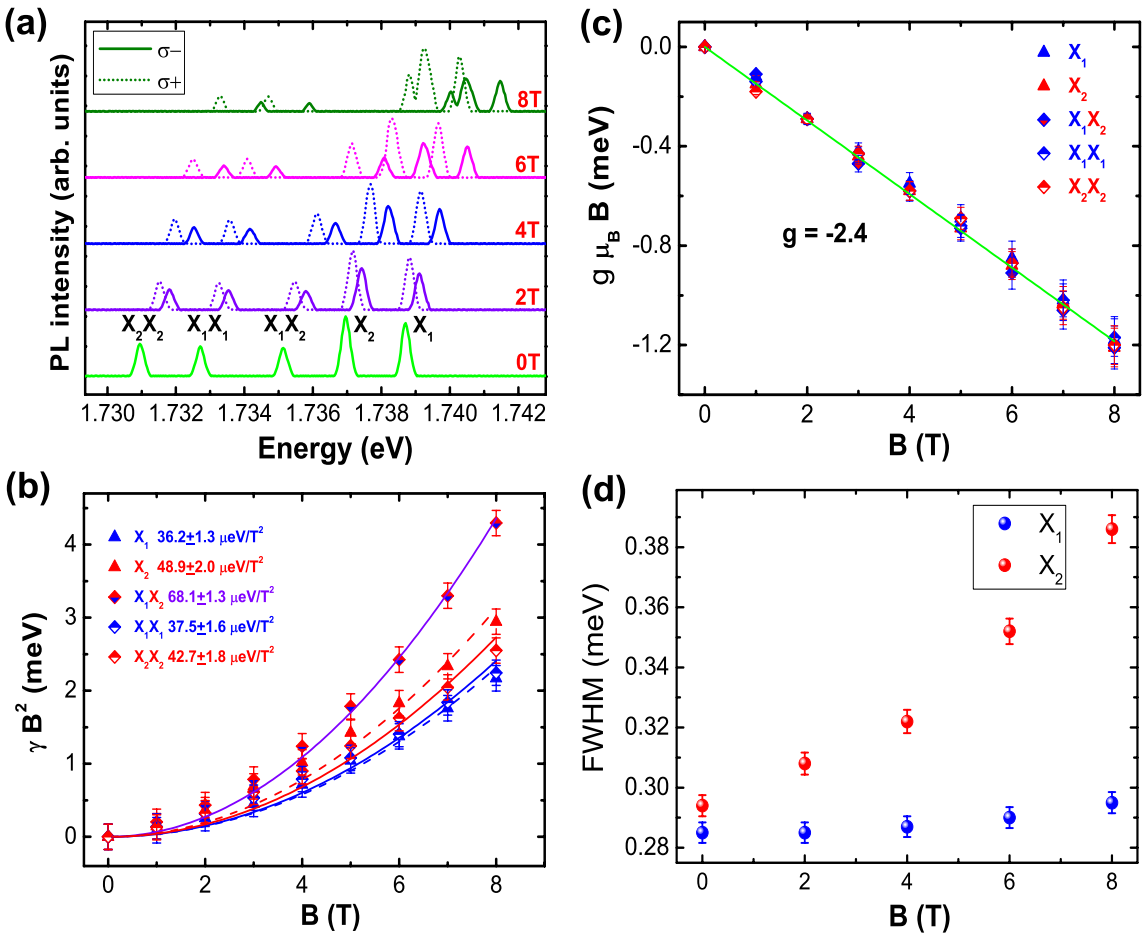

Figure 5: **(a)** Magneto-PL spectrum of excitons (X_1 and X_2), local biexcitons (X_1X_1 and X_2X_2), and coupled biexciton (X_1X_2) in a single lateral coupled-quantum-dot were measured up to 8 T with H-polarised excitation, whereby the diamagnetic coefficients (γ) **(b)** and the g-factor **(c)** were obtained. The PL linewidth of X_1 and X_2 for B were also compared **(d)**.

is also enhanced by FRET from X_1 to X_2, the $X_1X_2 - X_2$ transition is likely to be suppressed due to the saturation of the X_2 population. In this case, the super-linear PL growth of X_2 with excitation power ($\sim I_{ex}^{1.4}$) and the increased PL decay time of X_2 can be dominated by the FRET interaction. Nevertheless, it is still difficult to rule out the presence of the $X_1X_2 - X_1$ transition at the spectrally overlapped X_2 PL emission energy. A measurement of the different diamagnetic coefficients of biexcitons and excitons can be made by determining the spectral separation induced by the application of an external magnetic field (B).

As shown in Fig.5(a), the Zeeman-split magneto-PL spectra of the coupled biexcitons, local biexcitons, and excitons were measured up to 8 T with H-polarised excitation, whereby the diamagnetic coefficients ($\gamma = \frac{[E(\sigma^+)+E(\sigma^-)]/2-E(B=0)}{B^2}$) and the exciton g-factors ($g = [E(\sigma^+) - E(\sigma^-)]/\mu_B$) were obtained as shown in Fig. 5(b,c) from the PL energy of spins-parallel ($E(\sigma^+)$) and opposite ($E(\sigma^-)$) to B. Although the excitons, local biexcitons, and coupled biexcitons give the same g-factor ($g = -2.4$), it is noteable that the γ of the $X_1X_2 = 68.1 \pm 1.3 \mu eVT^{-2}$ is significantly larger than those of the excitons and local biexcitons. Because a diamagnetic coefficient is proportional to the wavefunction area,[29,30] the large γ of X_1X_2 implies that the wavefunction is probably extended across the two QDs. On the other hand, the wavefunctions of local biexcitons and excitons are isolated in a separate QD. As the γ of X_1X_1 ($37.5 \pm 1.6 \mu eVT^{-2}$) is comparable to that of X_1 ($36.2 \pm 1.3 \mu eVT^{-2}$), the two electrons and two holes of QD_1 are strongly correlated in the isolated range. When considering the small confinement area of QD_1 compared to that of QD_2, it is plausible that the γ of X_1 ($36.2 \pm 1.3 \mu eVT^{-2}$) and X_1X_1 ($37.5 \pm 1.6 \mu eVT^{-2}$) in QD_1 are smaller than those in QD_2. Interestingly, the γ of X_2 ($48.9 \pm 2.0 \mu eVT^{-2}$) is notably large, but is still less than the γ of $X_1X_2 - X_1$ transition but larger than that of X_2X_2 ($42.7 \pm 1.8 \mu eVT^{-2}$). Unfortunately, our spectral resolution is limited so that we cannot resolve the $X_1X_2 - X_2$ transition from X_2 PL spectrum. However, the PL linewidth measured near X_2 becomes significantly broadened compared to that of X_1 as shown in Fig. 5(d). Therefore, although the $X_1X_2 - X_2$ transition rate is small compared to $X_1X_2 - X_1$ transition, the incompletely

suppressed transition seems to still contribute. This might result in a spectral broadening within the X_2 spectral range.

In conclusion, we found that the exciton dipole-dipole interaction of a CQD becomes enhanced if the polarisation of non-resonant excitation is parallel to the coupling direction $[1\bar{1}0]$ (H-polarised excitation). We claim that the FRET interaction becomes dominant with increasing the H-polarised excitation, where redshifts, an exciton population transfer, and a coupled biexciton appear. We have also distinguished the coupled biexciton from local biexcitons by the large diamagnetic coefficient. One of the coupled biexciton transitions ($X_1X_2 - X_2$) was found to be spectrally overlapped with X_2. We conclude that $X_1X_2 - X_2$ is likely to be suppressed as a consequence of the exciton transfer from X_1 to X_2 but the suppression seems incomplete.

Acknowledgement

This work was supported by Korean Basic Science Research Program through the NRF funded by MEST (NRF-2014R1A1A2058789) and Pioneer Research (2013M3C1A3065522), and French-Korean LIA.

Supporting Information Available

The supporting information has details of the sample growth method, excitation dependence of the integrated PL and the time-resolved PL intensity of excitons (X_1 and X_2) and local biexcitons (X_1X_1 and X_2X_2) in QD_1 and QD_2 with H- and V-polarised excitation, and a theoretical model using the dipole-dipole interaction in a coupled-quantum dot structure. This material is available free of charge via the Internet at `http://pubs.acs.org/`.

References

(1) Bayer, M.; Hawrylak, P.; Hinzer, K.; Fafard, S.; Korkusinski, M.; Wasilewski, Z. R.; Stern, O.; Forchel, A. *Science* **2001**, *291*, 451.

(2) Sheng, W.; Leburton, J. P. *Phys. Rev. Lett.* **2002**, *88*, 167401.

(3) Bester, G.; Shumway, J.; Zunger, A. *Phys. Rev. Lett.* **2004**, *93*, 047401.

(4) Petta, J. R.; Johnson, A. C.; Taylor, J. M.; Laird, E. A.; Yacoby, A.; Lukin, M. D.; Marcus, C. M.; Hanson, M. P.; Gossard, A. C. *Science* **2005**, *309*, 2180.

(5) Robledo, L.; Elzerman, J.; Jundt, G.; Atature, M.; Hogele, A.; Falt, S.; Imamoglu, A. *Science* **2008**, *320*, 772.

(6) Weiss, K. M.; Elzerman, J. M.; Delley, Y. L.; Miguel Sanchez, J.; Imamoglu, A. *Phys. Rev. Lett.* **2012**, *109*, 107401.

(7) Villas-Bôas, J. M.; Govorov, A. O.; Ulloa, S. E. *Phys. Rev. B* **2004**, *69*, 125342.

(8) Emary, C.; Sham, L. J. *Phys. Rev. B* **2007**, *75*, 125317.

(9) Xu, X.; Williams, D. A.; Cleaver, J. R. A. *Appl. Phys. Lett.* **2005**, *86*, 012103.

(10) Rontani, M.; Amaha, S.; Muraki, K.; Manghi, F.; Molinari, E.; Tarucha, S.; Austing, D. G. *Phys. Rev. B* **2004**, *69*, 085327.

(11) Zhou, X. R.; Lee, J. H.; Salamo, G. J.; Royo, M.; Climente, J. I.; Doty, M. F. *Phys. Rev. B* **2013**, *87*, 125309.

(12) Doty, M. F.; Climente, J. I.; Korkusinski, M.; Scheibner, M.; Bracker, A. S.; Hawrylak, P.; Gammon, D. *Phys. Rev. Lett.* **2009**, *102*, 047401.

(13) Boyer de la Giroday, A.; Skold, N.; Farrer, I.; Ritchie, D. A.; Shields, A. J. *J. Appl. Phys.* **2011**, *110*, 083511.

(14) Ortner, G.; Bayer, M.; Lyanda-Geller, Y.; Reinecke, T. L.; Kress, A.; Reithmaier, J. P.; Forchel, A. *Phys. Rev. Lett.* **2005**, *94*, 157401.

(15) Kagan, C. R.; Murray, C. B. *Nature Nanotech.* **2015**, *10*, 1013.

(16) Stinaff, E. A.; Scheibner, M.; Bracker, A. S.; Ponomarev, I. V.; Korenev, V. L.; Ware, M. E.; Doty, M. F.; Reinecke, T. L.; Gammon, D. *Science* **2006**, *311*, 636.

(17) Wijesundara, K. C.; Rolon, J. E.; Ulloa, S. E.; Bracker, A. S.; Gammon, D.; Stinaff, E. A. *Phys. Rev. B* **2011**, *84*, 081404(R).

(18) Krenner, H. J.; Clark, E. C.; Nakaoka, T.; Bichler, M.; Scheurer, C.; Abstreiter, G.; Finley, J. J. *Phys. Rev. Lett.* **2006**, *97*, 076403.

(19) Wang, L.; Rastelli, A.; Kiravittaya, S.; Benyoucef, M.; Schmidt, O. G. *Adv. Mater.* **2009**, *21*, 2601.

(20) Unold, T.; Mueller, K.; Lienau, C.; Elsaesser, T.; Wieck, A. D. *Phys. Rev. Lett.* **2005**, *94*, 137404.

(21) Bayer, J.; Buyanova, I. A.; Suraprapapich, S.; Tu, C. W.; Chen, W. M. *Nanotechnology* **2009**, *20*, 375401.

(22) Bayer, J.; Buyanova, I. A.; Suraprapapich, S.; Tu, C. W.; Chen, W. M. *Journal of Physics* **2010**, *245*, 012044.

(23) Kim, H. D.; Kyhm, K.; Taylor, R. A.; Nogues, G.; Je, K. C.; Lee, E. H.; Song, J. D. *Appl. Phys. Lett.* **2013**, *102*, 033112.

(24) Liang, B.; Wang, Z.; Wang, X.; Lee, J.; Mazur, Y. I.; Shih, C.; Salamo, G. J. *ACS Nano* **2008**, *2*, 2219.

(25) Kim, I.; Kyhm, K.; Kang, M.; Woo, H. Y. *J. Lumin.* **2014**, *149*, 185.

(26) Kim, H. D.; Kyhm, K.; Taylor, R. A.; Nicolet, A. A. L.; Potemski, M.; Nogues, G.; Je, K. C.; Lee, E. H.; Song, J. D. *Appl. Phys. Lett.* **2013**, *103*, 173106.

(27) Lakowicz, J. R. *Springer, New York,* **2006**, *3rd*.

(28) Kim, I.; Kiba, T.; Murayama, A.; Song, J. D.; Kyhm, K. *Curr. Appl. Phys.* **2015**, *15*, 733.

(29) Lin, T.-C.; Lin, C.-H.; Ling, H.-S.; Fu, Y.-J.; Chang, W.-H.; Lin, S.-D.; Lee, C.-P. *Phys. Rev. B* **2009**, *80*, 081304(R).

(30) Kim, H. D. et al. *Nano Lett.* **2016**, *16*, 27.

Graphical TOC Entry